

Passive coherent location radar systems. Part 1: Performance prediction

H.D. Griffiths and C.J. Baker

Abstract: Passive coherent location (PCL) systems are a variant of bistatic radar that exploit ‘illuminators of opportunity’ as their sources of radar transmission. Dispensing with the need for a dedicated transmitter makes PCL inherently low cost, and hence attractive for a broad range of applications. Although a number of experimental and development examples exist, relatively little has been reported on the detailed performance of these systems and the resulting effects that these will have on the interpretation of backscatter and exploitation of derived information. In the paper a bistatic form of the radar range equation specifically tailored to PCL systems is developed. Realistic examples are used to examine and compare variations in sensitivity and coverage for three candidate transmitters of opportunity. These are analogue FM radio, cellular phone base stations and digital audio broadcast (DAB). These examples show that a wide and extremely useful set of detection ranges are achievable and also highlight some of the key issues underpinning more detailed aspects of predicting detection performance.

1 Introduction

The very earliest radar systems were bistatic, with the transmitter and receiver at separate locations [1]. The advent of the duplexer, which permitted simplicity of operation in addition to cost and space savings, has meant that transmitting and receiving through the same antenna (monostatic radar) has since dominated radar design. However, bistatic radar has a number of advantages that have continued to make it of interest, and now practical systems are beginning to emerge. The principal advantages of bistatic radar are (i) the fact that the receiver is passive, making it far less vulnerable to electronic counter measures (ECM) and (ii) it is a counter to stealth technology, which is designed primarily to defeat monostatic radar. In addition multiple receivers can be employed, each one forming a bistatic radar with the single transmitter. This offers the potential for tailored coverage and a richer information source to enable more accurate location, high resolution imaging and target reconstruction. The price to be paid for these advantages is an increase in system complexity and processing. In particular synchronisation and beam pointing are more difficult to implement and have probably held back the take up of bistatic radar. However, there have been a number of recent improvements in technology that help to address the extra complexities of bistatic radar. These include high speed digital signal processors (DSP), phased array antennas, and the deployment of GPS satellite navigation systems, which can be used for synchronisation.

More recently there has been an upsurge of interest in bistatic radar systems that exploit illuminators of opportunity (also known as ‘passive radar’ or ‘passive coherent location’). This is attractive as it can reduce dramatically the costs of the system hardware. The rapid growth in the number of RF emissions for TV and radio broadcasts in addition to terrestrial and space based communications has resulted in a wide range of signal types available for exploitation by passive radar. Further, many such transmissions are at VHF and UHF frequencies, which allows these parts of the spectrum not normally available for radar use, and at which stealth treatment of targets may be less effective, to be used. However, the location of the transmitter and the form of the transmission to be exploited are no longer under the control of the radar designer. The multiplicity of transmissions from both terrestrial [2] and space based sources [3, 4] provide spatial and frequency diversity and can be exploited to further improve detection performance. Examples of reported operational systems include the Lockheed Martin ‘Silent Sentry’ system for air and space surveillance [2], the Roke Manor Research CELLDAR system for air target detection [5] and the Manastash Ridge radar for atmospheric and ionospheric studies [6]. Other reported experimental systems include those proposed by Dynetics [7] and UCL [8–10]. Applications include air-space surveillance [2, 5], maritime surveillance [10], atmospheric studies [6], ionospheric studies [6], oceanography [11], mapping lightning channels in thunderstorms [12] and monitoring radioactive pollution [13]. There have also been recent reports of algorithm development for interferometry [14], target tracking [15] and target classification [15, 16]. This range and diversity of systems and applications is indicative of the increasing importance of this form of sensor system.

However, there have been relatively few publications [7–9, 15, 17, 18] describing detailed aspects of system performance such as waveform properties and real geometrical factors, and almost nothing on the impact these features may have on the overall system capability. In this paper we examine the factors that affect the detection performance of passive coherent location radar systems.

© IEE, 2005

IEE Proceedings online no. 20045082

doi: 10.1049/ip-rsn:20045082

Paper first received 20th September 2004 and in final revised form 12th April 2005

The authors are with University College London, Department of Electronic and Electrical Engineering, Torrington Place, London, WC1E 7JE, UK

E-mail: h.griffiths@ee.ucl.ac.uk

Equally important in PCL are the properties of the waveform to be exploited. Part 2 of this paper [19] considers the associated issues of the form and variability of the ambiguity functions of passive radar signals and discusses how these further effect the performance and applications of PCL.

2 The radar equation for passive radar systems

2.1 The bistatic radar equation

The starting point for an analysis of the performance of a passive radar system is the well-known bistatic radar equation:

$$\frac{P_r}{P_n} = \frac{P_t G_t}{4\pi r_1^2} \cdot \sigma_b \cdot \frac{1}{4\pi r_2^2} \cdot \frac{G_r \lambda^2}{4\pi} \cdot \frac{1}{kT_0 B F} \cdot L \quad (1)$$

where

| | |
|--------------|--|
| P_r | is the received signal power |
| P_n | is the receiver noise power |
| P_t | is the transmit power |
| G_t | is the transmit antenna gain |
| r_1 | is the transmitter-to-target range |
| σ_b | is the target bistatic radar cross-section |
| r_2 | is the target-to-receiver range |
| G_r | is the receive antenna gain |
| λ | is the signal wavelength |
| k | is Boltzmann's constant |
| T_0 | is the noise reference temperature, 290 K |
| B | is the receiver effective bandwidth |
| F | is the receiver effective noise figure |
| $L (\leq 1)$ | are system losses |

In using this equation to predict the performance of a passive radar system it is critical to understand the correct value of each of these parameters that is to be used. Signal parameters for typical passive radar illumination sources are summarised in Table 1.

The transmit power P_t is substantial for many passive radar sources, since broadcast and communications receivers often have inefficient antennas and poor noise figures and the transmission paths are often far from line-of-sight; thus the transmit powers have to be significantly higher to overcome the inefficiencies and losses. In the UK, the highest power FM radio transmissions are 250 kW (ERP) per channel, with many more of lower power [20].

The highest power analogue TV transmissions are 1 MW (ERP) per channel [20]. These are omnidirectional in azimuth, and are sited on tall masts on high locations to give good coverage. The vertical-plane radiation patterns are tailored to avoid wasting too much power above the horizontal.

GSM cellphone transmissions in the UK are in the 900 MHz and 1.8 GHz bands. The modulation format is such that the downlink and uplink bands are each of 25 MHz bandwidth, split into 125 FDMA channels each of 200 kHz bandwidth, and a given base station will only use a small number of these channels. Each channel carries 8 signals via TDMA, using GMSK modulation. Third generation (3G) transmissions are in the 2 GHz band, using CDMA modulation over 5 MHz bandwidth. The radiation patterns of cellphone base station antennas are typically arranged in 120° azimuth sectors, and shaped in the vertical plane again to avoid wasting power. The pattern of frequency re-use means that there will be cells using the same frequencies within quite short ranges. Licensed ERPs are typically in the region of 400 W, although in many cases the actual transmit powers are lower. The OFCOM sitefinder website [21] gives details of the location and operating parameters of each basestation throughout the UK, and an example of the information provided by this website is shown in Table 2.

While the figures quoted in the paragraph above relate to the UK, the figures for other countries will be comparable.

In all cases it is necessary to consider the power in the portion of the signal spectrum used for passive radar purposes, which may not be the same as the power of the total signal spectrum. For example the ambiguity properties of the full signal may not be as favourable as those of a portion of the signal. This is the case for an analogue television transmission; the full signal has pronounced ambiguities associated with the 64 μ s line repetition rate, but better ambiguity performance may be realised by taking just a portion of the signal spectrum at the expense of reduced signal power.

2.2 Target bistatic radar cross-section

In PCL target detection and location are a function of the spatially dependent bistatic RCS and target dynamics, as well as the radar design parameters. Targets can be detected in range, Doppler and angle using conventional processing approaches. The target bistatic radar cross-section σ_b will not in general be the same as the monostatic cross-section,

Table 1: Signal parameters for typical passive radar illumination sources

| Transmission | Frequency | Modulation, bandwidth | $P_t G_t$ | Power density (Wm^{-2}) $\Phi = (P_t G_t)/4\pi r_1^2$ |
|-----------------------------|------------------|--|-------------|---|
| HF broadcast | 10–30 MHz* | DSB AM, 9 kHz | 50 MW | –67 to –53 dBW m^{-2} at $r_1 = 1000$ km |
| VHF FM (analogue) | ~ 100 MHz | FM, 50 kHz | 250 kW [20] | –57 dBW m^{-2} at $r_1 = 100$ km |
| UHF TV (analogue) | ~ 550 MHz | vestigial-sideband AM (vision); FM (sound), 5.5 MHz | 1 MW | –51 dBW m^{-2} at $r_1 = 100$ km |
| Digital audio broadcast | ~ 220 MHz | digital, OFDM 220 kHz | 10 kW | –71 dBW m^{-2} at $r_1 = 100$ km |
| Digital TV | ~ 750 MHz | digital, 6 MHz | 8 kW | –72 dBW m^{-2} at $r_1 = 100$ km |
| Cellphone basestation (GSM) | 900 MHz, 1.8 GHz | GMSK, FDM/TDMA/FDD 200 kHz | 100 W [21] | –81 dBW m^{-2} at $r_1 = 10$ km |
| Cellphone basestation (3G) | 2 GHz | CDMA 5 MHz | 100 W | –81 dBW m^{-2} at $r_1 = 10$ km |

*Appropriate frequency will depend on time of day.

Table 2: Example attributes of a mobile phone basestation located to the northern end of Gower Street in London, UK

| | |
|-------------------------|----------|
| Name of operator | T-Mobile |
| Operator site reference | 98463 |
| Height of antenna | 35.8 m |
| Frequency range | 1800 MHz |
| Transmitter power | 26 dBW |
| Maximum licensed power | 32 dBW |
| Type of transmission | GSM |

though for non-stealthy targets the range of values may be comparable [17, 22]. However, rather little has appeared in the open literature as to the bistatic radar cross-section of targets and this remains an area for future research. In addition there have been only a few published reports of bistatic clutter measurements [e.g. 23–25] and a much more complete treatment is required to enable more realistic calculations of PCL performance.

As the bistatic angle is increased to 180° the forward scatter region is encountered. In this region target cross-sections can be considerably enhanced. This is explained by Babinet's principle, which means that the forward scatter from a perfectly-absorbing target is the same (apart from a 180° phase shift) as that from a target-shaped aperture in a perfectly-conducting sheet, which for a target of physical cross-sectional area A gives a radar cross-section of

$$\sigma_b = \frac{4\pi A^2}{\lambda^2} \quad (2)$$

The angular width of the scattered signal in the horizontal or vertical plane is given by

$$\theta_b = \frac{\lambda}{d} \quad (3)$$

where d is the target linear dimension in the appropriate plane. Figure 1 plots the dependence of σ_b and θ_b on frequency, for a target with $A = 10 \text{ m}^2$ and $d = 20 \text{ m}$, showing that θ_b increases with frequency as the forward scatter is concentrated into an increasingly narrow beam. This implies that low frequencies are more favourable for the exploitation of forward scatter, so that target detection may be achieved over an adequately wide angular range. Forward scatter does not enable range to be measured directly; however, target location can be estimated using a combination of Doppler and bearing as explained in [26].

Another mechanism for enhancement of bistatic RCS of aircraft targets is specular reflection from the underside of

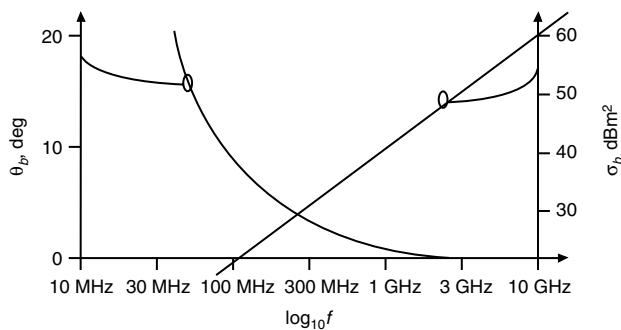


Fig. 1 Variation of RCS σ_b and angular width θ_b of forward scatter of a target of physical area 10 m^2 and linear dimension 20 m , against frequency

the aircraft. This, though, would depend on the specular condition being met and would therefore be ephemeral in nature. This may improve the sensitivity to elevated targets, given that most transmitters direct their signals towards the Earth's surface.

2.3 Receiver noise figure

The noise and interference level against which the wanted signal must compete for detection is made up of several components. These may be visualised in the form of a two dimensional function $P_i(\theta, f)$ of direction and frequency. These components are as follows:

- (i) The basic noise figure of the receiver, which at VHF or UHF will be of the order of a few dBs at most; the noise power will be uniformly distributed over θ and f ;
- (ii) The direct signal from the bistatic transmitter. This will be the dominant component, and will occur at the appropriate incidence angle and occupy the appropriate bandwidth;
- (iii) Multipath versions of the direct signal (i.e. clutter), each of a particular signal level and at a particular incidence angle, and possibly time-varying and Doppler-shifted;
- (iv) Direct and multipath versions of other co-channel transmissions;
- (v) Other signals due to (for example) radiation from computers, impulsive or spurious signals.

Unless steps are taken to suppress these components, the sensitivity and dynamic range of the system will be severely limited.

Measurements were made of the signal and noise environment in the VHF broadcast band around 100 MHz in central London, using a vertically-polarised dipole antenna mounted outside the 10th floor of the University College London Engineering Sciences Faculty building. A typical spectrum is provided in Fig. 2, which shows direct signal levels of the order of -45 dBm , and a noise level (in between the broadcast signals) of the order of -90 dBm in 30 kHz.

This result is important, because it shows that the signal and noise environment can be severe. In the example of Fig. 2 the noise level is some 40 dB greater than thermal noise, and the direct signals are some 45 dB greater still. The effective value of noise figure to be used in (1) will depend on the particular signal and noise environment and on the degree of suppression that can be obtained. Whilst the example of Fig. 2 is severe, lower noise levels might be expected in suburban and rural environments, and at the higher frequencies used by television and cellphone transmission; nevertheless, an effective noise figure of 25 dB is not pessimistic.

We can formulate a simple expression for the amount of direct signal suppression required by calculating the ratio of the indirect received signal to the direct signal and requiring this to be at least the same value as that used to compute the maximum detection range. We make the simple assumption that a target can be seen above this level of direct signal breakthrough and hence that it approximates to the highest level of interference that is tolerable for single 'pulse-like' detection. There is, however, no benefit from integration as the direct leakage will also integrate up, and this may lead to a more stringent requirement needing to be set in practice. This places the direct leakage signal at the same level as the noise floor in the receiver and hence it has the attractive feature of proving equivalent performance to 'single-pulse' detection. Thus to achieve adequate suppression

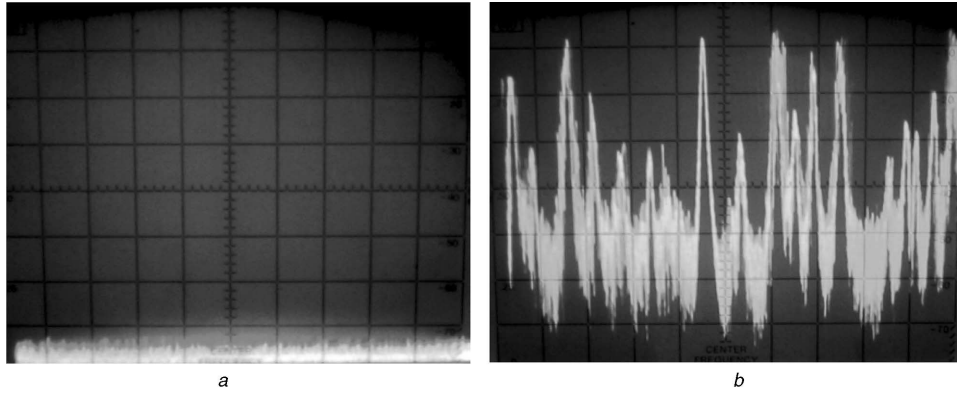


Fig. 2 Noise levels in a passive radar receiver

a Thermal noise in 30 kHz bandwidth corresponding to 5 dB receiver noise figure
b Signal and noise levels measured from 10th floor of UCL in Central London.
 Horizontal scale 95–100 MHz; vertical scale 10 dB/division; top of screen = -40 dBm

and hence maintenance of full system dynamic range the direct signal must be cancelled by an amount given by the magnitude of the ratio of the indirect and directly received signals, e.g.

$$\frac{P_r}{P_d} = \frac{r_b^2 \sigma_b}{4\pi r_1^2 r_2^2} > \frac{P_r}{P_d} \quad (4)$$

where P_r is the target echo signal, P_d is the direct signal, and r_b is the transmitter-to-receiver range (bistatic baseline). This expression is indicative only and, strictly speaking, the direct signal should be below that of the noise floor after integration, if integration is employed.

Taking the numerical example of a television transmitter located at Crystal Palace in the south of London, a receiver located at University College London, and assuming a 1 m² target and a maximum detection range of 40 km, this equates to a requirement for suppression of direct signal leakage of some 120 dB, if this is to be taken down to thermal noise level. It should be noted that as the detection range is reduced from the maximum the amount of direct signal breakthrough compared to the indirect signal will fall sharply. In addition the leakage signal will be time varying and subjected to multiple scattering paths. This behaviour requires a thorough and detailed understanding to optimise the performance of a given design.

There are several techniques that may be used to suppress this leakage. These include: (i) physical shielding, (ii) Doppler (Fourier) processing, (iii) high gain antennas, (iv) sidelobe cancellation, (v) adaptive beamforming and (vi) adaptive filtering. Each one of these techniques will provide different suppression characteristics over the (θ, f) plane, thus physical shielding or beamforming techniques will provide suppression as a function of θ , Doppler processing or adaptive filtering will provide suppression as a function of f . The combination of high gain antennas and adaptive beamforming also enables multiple simultaneous transmissions to be exploited.

The Manastash Ridge radar [6] provides an example of the use of physical shielding; in this case suppression is achieved by siting the receiver on the other side of a large mountain that provides the screening. In other cases some simpler more localised methods may be used such as appropriate deployment of radar absorbing material (RAM).

For the detection of moving targets Doppler or Fourier processing will automatically improve dynamic range, as the direct signal leakage will only occur at DC (with some spill over). However it should be noted that significant

sidelobe leakage owing to inadequate suppression of very strong directly received signals will reduce the gain from Fourier processing and hence impair dynamic range.

In the numerical example above, an omnidirectional antenna was assumed. In practice it is much more likely that an array antenna will be used and advantage can be taken of all of the techniques (iii) to (v). This allows the directional gain of the antenna to provide suppression via control of the sidelobes. If a fully digital antenna is employed then adaptive beamforming can be used to minimise sensitivity in the direction of the location of the directly received signal. If external noise such as multipath is present then multiple nulls have to be formed. If the external noise environment is non-stationary, the cancellation will need to be adaptive, with a suitably rapid response time. The number of degrees of freedom, and hence the number of antenna elements and receiver channels, must be greater than the number of signal components to be suppressed. The antenna pattern factor, the transmitter and receiver locations and the target trajectory for a given scenario will lead to ‘blind zones’. These are caused either by a loss of line of sight between the transmitter, target and receiver or when the target crosses the bistatic baseline between the transmitter and receiver. Ambiguities will also arise owing to these geometrical relationships and are highlighted in Part 2 of this paper [19].

It may also be useful to use a stage of analogue cancellation to reduce the dynamic range requirement of subsequent digital cancellation. In either case standard adaptive filtering techniques can be used. We can say that a combination of techniques (e.g. physical screening, Doppler processing, and adaptive cancellation) will be needed to achieve the high levels of suppression required. However, the use of an array antenna and adaptive cancellation processing does mean that the receiving system is not as simple nor as cheap as might originally have been supposed, so the claims that are made for PCL in this respect should be suitably tempered.

2.4 Effective bandwidth and integration gain

In a PCL system the direct signal is used as a reference against which the indirect or reflected signal can be correlated to provide processing gain for sensitivity and bandwidth for resolution via its modulation content. The effective receiver bandwidth B is that of the directly received signal. This bandwidth is subject to the processing gain owing to coherent integration, which in turn depends

on the time for which the target echoes remain coherent. A rule of thumb for the maximum value of the coherent processing gain is

$$T_{MAX} = \left(\frac{\lambda}{A_R} \right)^{1/2} \quad (5)$$

where A_R is the radial component of target acceleration. Hence the maximum processing gain is

$$G_p = T_{MAX} B \quad (6)$$

For example, with a VHF FM radio waveform of bandwidth 50 kHz and an integration time of 1 second, the processing gain will be 37 dB. From this, the bistatic radar equation can be re-cast in the following form:

$$(r_2)_{max} = \left(\frac{\Phi \sigma_b G_r \lambda^2 L G_p}{(4\pi)^2 (S/N)_{min} k T_0 B F} \right)^{1/2} \quad (7)$$

This predicts the coverage around the transmitter and receiver in the form of the well known Ovals of Cassini (loci corresponding to $r_1 r_2 = \text{constant}$). This is the form of the bistatic radar equation that will be used to predict the performance for differing illuminators of opportunity in the following Section.

3 Performance prediction

All of the foregoing has shown that some care must be taken in using the bistatic radar equation to predict the performance of passive radar systems. In this Section we present performance predictions for three 'straw man' systems, attempting to show the likely achievable performance and to identify critical factors. The systems considered are FM radio, cellphone basestations and digital radio. In each case an omnidirectional receive antenna, a target RCS of 1 m^2 , a noise figure of 25 dB, losses of 5 dB and 0.1 s integration time are assumed.

3.1 FM radio

FM radio transmissions have the inherent attractive properties of very broad coverage and relatively high transmitter powers. For the example considered in this paper the transmitter at Wrotham in the south-east of England is taken together with a receiver sited at the Engineering Sciences Faculty building of UCL. The transmitted power is 250 kW and broadcasts are made in the frequency range 89.1–93.5 MHz. Figure 3 shows a plot of the detection range; the contour represents a signal-to-noise ratio of 15 dB (and this value of signal-to-noise ratio is used for all subsequent Figures of this type). The modulation bandwidth is taken as 55 kHz, which is considerably less than specified for these transmissions. As is demonstrated in Part 2 of this paper [19] the modulation bandwidth is a function of programme content and therefore varies with time, and 55 kHz represents a typical value. A signal-to-noise ratio of 15 dB or greater is maintained out to a range of nearly 30 km. This performance is constrained by the effective noise figure of the receiver, and better performance would be obtained with better suppression of direct signal and noise. It should be noted that the power emitted by transmitters across the UK varies from as little as 4 W to a maximum of 250 kW and of course this variation has to be factored in carefully to performance predictions. Figure 4 shows how the detection range varies when a second

transmitter is exploited. Here the transmitter at Crystal Palace, which has a transmit power of 4 kW, is exploited. The range of coverage is proportionally less as there is approximately 18 dB less transmitted power and the signal-to-noise ratio of 15 dB is limited to around a little over 10 km. Figure 5 illustrates how the coverage changes when the two transmitters are exploited together using non-coherent integration. Now the detection range is extended to over 30 km. However, an alternative is to process the detections from each transmitter independently and then combine them as this is simpler. Coherent combination is unlikely as the transmissions will probably be at differing frequencies and not synchronised. Overall the high transmit powers and good coverage make FM radio transmissions particularly well suited to air target detection for both civil and military applications. Equally they could be used for marine navigation in coastal waters although clutter may be a more significant problem.

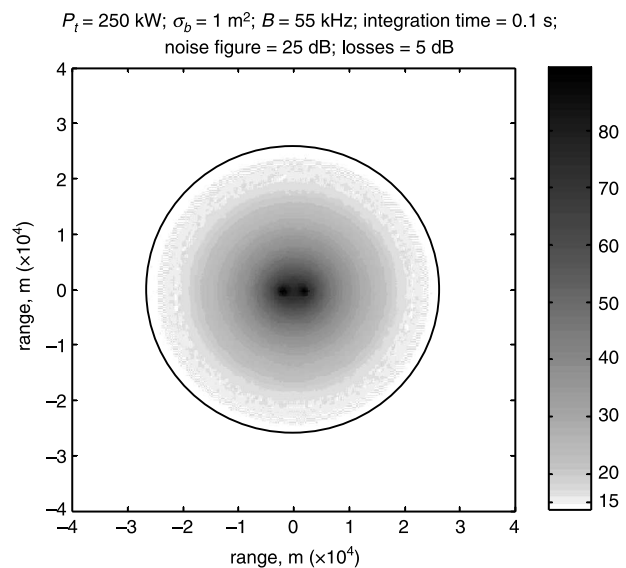


Fig. 3 Detection range for an FM radio transmitter at Wrotham in south-east England and a receiver at UCL

The solid contour represents a signal-to-noise ratio of 15 dB

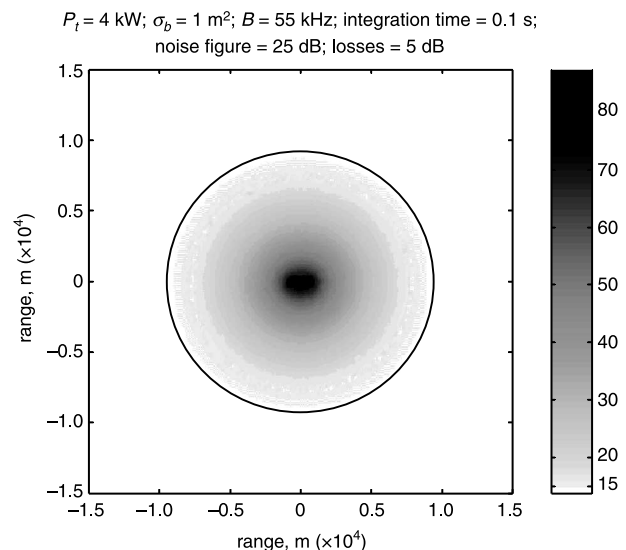


Fig. 4 Detection range for an FM radio transmitter at Crystal Palace and a receiver at UCL

The solid contour represents a signal-to-noise ratio of 15 dB

$P_t = 250 \text{ kW}$, 4 kW ; $\sigma_b = 1 \text{ m}^2$; $B = 55 \text{ kHz}$; integration time = 0.1 s ;
noise figure = 25 dB ; losses = 5 dB

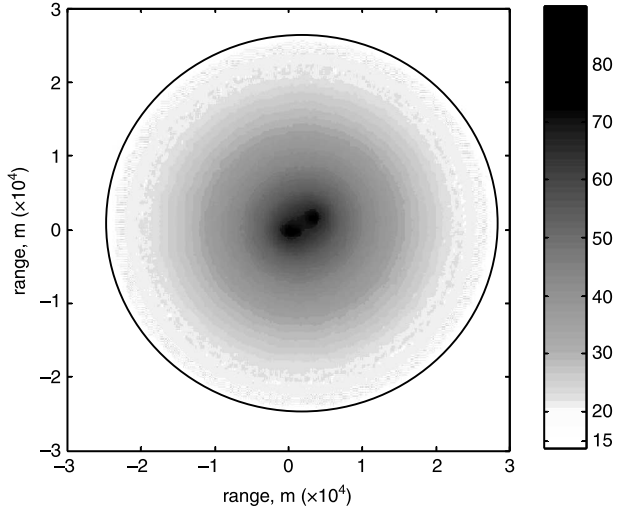


Fig. 5 Detection range for FM radio transmitters at Wrotham and Crystal Palace and a receiver at UCL

The solid contour represents a signal-to-noise ratio of 15 dB

$P_t = 10 \text{ kW}$; $\sigma_b = 1 \text{ m}^2$; $B = 200 \text{ kHz}$; integration time = 0.1 s ;
noise figure = 25 dB ; losses = 5 dB

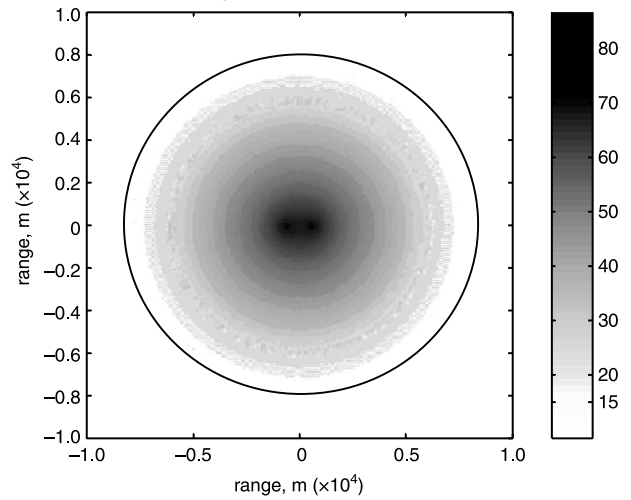


Fig. 7 Detection range for a DAB transmitter at Crystal Palace and a receiver at UCL

The solid contour represents a signal-to-noise ratio of 15 dB

3.2 Cellphone basestations

The second system uses a cellphone basestation transmitter with the parameters listed in Table 2. This particular transmitter has an operating frequency of 1800 MHz and is located towards the northern end of Gower Street approximately 200 m from the engineering building of UCL where the receiver is again placed. The other parameters are maintained constant as with the first case. A plot of the detection range is shown in Fig. 6, which suggests a maximum range of around 1.2 km , although better performance would be obtained with better suppression of noise and direct signals, and with higher receive antenna gain. Clearly this is much less than for the first example, and would seem therefore to have more limited application. However, as there is such an extensive and diverse network of basestations, targets could be tracked though such a network and hence the coverage

$P_t = 400 \text{ W}$; $\sigma_b = 1 \text{ m}^2$; $B = 55 \text{ kHz}$; integration time = 0.1 s ;
noise figure = 25 dB ; losses = 5 dB

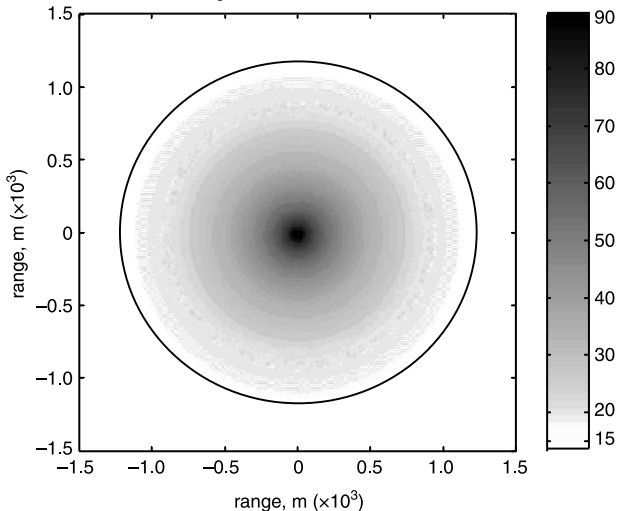


Fig. 6 Detection range for a mobile phone basestation located at the northern end of Gower Street in central London and a receiver at UCL

The solid contour represents a signal-to-noise ratio of 15 dB

may be extended greatly encompassing the area covered by the network itself. This extends the range of application to include those such as counting of vehicles for traffic flow management and remote monitoring of movement around buildings as a security device, possibly acting as a cue for a camera system.

3.3 Digital radio

The third example uses a digital audio broadcast transmission from Crystal Palace in south London. This has a transmit power of 10 kW . Figure 7 shows the detection range. As might be expected for a high power transmitter of this type the coverage is out to a range of around 9 km . Thus despite the higher transmit power than for the FM transmission the maximum detection range is shorter. This is due to the higher frequency offsetting the lower transmit power. Again it should be noted that output powers of transmissions of this kind vary between 500 W and 10 kW . Additionally coverage is not currently as universal as is the case for FM transmissions although new transmitters are constantly being added.

One of the strengths of PCL is that several different types of emission of opportunity could be exploited at a single receiver site. This has the advantage of providing frequency diversity and spatial diversity and as such makes PCL somewhat equivalent to a multi-site or netted radar system (i.e. multiple transmitter locations and a single receiver). There are also a number of aspects of performance that have not yet been considered. For example, FM transmissions have been used to probe the ionosphere and therefore might be expected to have useful height coverage but mobile phone basestations deliberately concentrate their emissions towards the ground and may not necessarily have such good coverage of higher altitude aircraft. Another factor that has to be considered carefully is integration time. We have assumed an integration time of 0.1 second and that the integration is 100% efficient. In practice targets will de-correlate and the integration efficiency will be less. A reasonable assumption might be for a reduction in signal-to-noise ratio of 3 dB . Implementation of a Doppler tracking filter could improve upon this. In estimating performance potential it is advisable to adopt a slightly conservative

approach when choosing values for the parameters comprising the system. Indeed performance calculations of this type are only indicative, especially as they do not include a full treatment of losses, the environment and clutter properties. Ultimately these and other aspects of performance do not lend themselves well to modelling and real systems will have to be constructed and tested.

4 Conclusions

In this paper we have re-cast the bistatic radar equation into a form that readily reflects the design features of a PCL system. This highlights the importance of the bistatic geometry and the key dependence on the nature of the illuminating waveform. The form and nature of bistatic target and clutter reflections are not well known and require extensive further research. We have shown that the noise and signal environment for a PCL receiver can be severe, and that appropriate suppression of direct signals and noise will be necessary. Even then, the radar equation should use an appropriate value of noise figure to predict detection performance. A 'rule of thumb' expression has been presented that indicates the high levels of direct signal suppression that are required to ensure that maximum detection ranges can be achieved. It should be noted that in single-frequency networks such as DAB, the suppression of co-channel signals is even more complicated.

Prediction of detection range and coverage for a variety of illuminators of opportunity shows that detection ranges of several tens of kilometres are readily achievable. It should be emphasised that these results have been computed for a 1 m² target and have taken fairly pessimistic estimates for the receiver noise figure; larger targets, better suppression of the noise and direct signals, and receive antenna gains of greater than unity will give better results. Performance is highly dependent on the properties of the illuminator. However, it is expected that full scale systems will have a performance at least as good as the levels predicted here. Thus PCL may be invoked to support quite a wide range of applications provided they are consistent with the limitations imposed by the availability of illuminators. Indeed the plethora of radio frequency radiation sources will undoubtedly increase still further and the case for PCL becomes ever more compelling. Further more sophisticated processing techniques such as SAR, ISAR, interferometry and others can all be exploited. In the second part of this paper we examine these properties in much more detail. This allows ambiguity function properties to be evaluated and examined. In this way further realism can be applied to predictions of actual radar performance and consequently a sound foundation for a much more comprehensive approach to PCL system design can be established.

5 References

- Willis, N.C.: 'Bistatic radar' (Artech House, 1991)
- Baniak, J., Baker, G., Cunningham, A.M., and Martin, L.: 'Silent Sentry passive surveillance', *Aviat. Space Technol.*, 7 June 1999
- Cherniakov, M., Nezhlin, D., and Kubin, K.: 'Air target detection via bistatic radar based on LEOS communication systems', *IEE Proc., Radar Sonar Navig.*, 2002, **149**, (1), pp. 33–38
- Griffiths, H.D., Baker, C.J., Baubert, J., Kitchen, N., and Treagust, M.: 'Bistatic radar using spaceborne illuminator of opportunity'. Proc. RADAR 2002 Conf., Edinburgh; IEE Conf. Publ., **490**, October 2002, pp. 1–5, 15–17
- <http://www.roke.co.uk/sensors/stealth/cellradar.asp>
- Sahr, J.D., and Lind, F.D.: 'The Manastash Ridge radar: a passive bistatic radar for upper atmospheric radio science', *Radio Sci.*, 1997, **32**, (6), pp. 2345–2358
- Zoeller, C.L., Budge, Jr., M.C., and Moody, M.: 'Passive coherent location radar demonstration'. Proc. Thirty-Fourth Southeastern Symp. on System Theory, 18–19 March 2002, pp. 358–362
- Griffiths, H.D., and Long, N.R.W.: 'Television based bistatic radar', *IEE Proc. F, Commun. Radar Signal Process.*, 1986, **133**, (7), pp. 649–657
- Griffiths, H.D., Garnett, A.J., Baker, C.J., and Keaveny, S.: 'Bistatic radar using satellite illuminators of opportunity'. Proc. RADAR Conf., Brighton, IEE Conf. Publ. 365, 12–13 October 1992, pp. 276–279
- Griffiths, H.D.: 'From a different perspective: principles, practice and potential of bistatic radar'. Proc. Int. Conf. RADAR 2003, Adelaide, Australia, 3–5 September 2003, pp. 1–7
- Trizna, D., and Gordon, J.: 'Results of a bistatic HF radar surface wave sea scatter experiment'. Proc. IGARSS, Vol. 3, 24–28 June 2002, pp. 1902–1904
- Grenaker, E.F., and Geisheimer, J.L.: 'The use of passive radar for mapping lightning channels in a thunderstorm'. Proc. IEEE Radar Conf., 5–8 May 2003, pp. 28–33
- Yakubov, V.P., Antipov, V.B., Losev, D.N., and Yuriev, I.A.: 'Passive radar detection of radioactive pollution'. Application of the Conversion Research Results for International Cooperation, SIBCONVERS. The Third Int. Symp., **2**, May 18–20, 1999, pp. 397–399
- Meyer, M., and Sahr, J.D.: 'Passive coherent radar scatter interferometer implementation, observations and analysis', *Radio Sci.*, 2004, **39**, RS3008, doi: 0.1029/2003RS002985
- Herman, S., and Moulin, P.M.: 'A particle filtering approach to passive radar tracking and automatic target recognition'. IEEE Aerospace Conf. Proc., 9–16 March 2002, **4**, pp. 4-1789–4-1808
- Elirman, L.M., and Lanterman, A.D.: 'A robust algorithm for automatic target recognition using passive radar'. Proc. Thirty-Sixth Southeastern Symp. on System Theory, 14–16 March, 2004, pp. 102–106
- Jackson, M.C.: 'The geometry of bistatic radar systems', *IEE Proc. F, Commun. Radar Signal Process.*, 1986, **133**, (7), pp. 604–612
- Willis, N.C.: 'Bistatic radar', in Skolnik, M.I., (Ed.): 'Radar handbook', (McGraw-Hill, 1990, 2nd edn), Chap. 25
- Baker, C.J., Griffiths, H.D., and Papoutsis, I.: 'Passive coherent radar systems - Part II: waveform properties', *IEE Proc., Radar Sonar Navig.*, 2005, **152**, (3), pp. 160–168
- <http://www.bbc.co.uk/reception/>
- <http://www.sitefinder.radio.gov.uk/>
- Kell, R.E.: 'On the derivation of bistatic RCS from monostatic measurements', *Proc. IEEE*, 1965, **53**, pp. 983–988
- Larson, R.W., Maffett, A.L., Heimiller, R.C., Fromm, A.F., Johansen, E.L., Rawson, R.F., and Smith, F.L.: 'Bistatic clutter measurements', *IEEE Trans. Antennas Propag.*, 1978, **AP-26**, (6), pp. 801–804
- Wicks, M., Stremmer, F., and Anthony, S.: 'Airborne ground clutter measurement system design considerations', *IEEE Aerosp. Electron. Syst. Mag.*, 1988, pp. 27–31
- McLaughlin, D.M., Boltmew, E., Wu, Y., and Raghavan, R.S.: 'Low grazing angle bistatic NRCS of forested clutter', *Electron. Lett.*, 1994, **30**, (18), pp. 1532–1533
- Howland, P.E.: 'Target tracking using television based bistatic radar', *IEE Proc., Radar Sonar Navig.*, 1999, **146**, (3), pp. 166–174